Hybridization Through Modularity: Exploring Complex Modes of Locomotion with a "Bag of Robotic Modules"

Yuanmeng Huang[1], Jonathan Miller[1], Upinder Kaur[1], Yubing Han[1], Ram M.S. Ramdas[2], Shashank Priya[2], and Richard M. Voyles[1]

[1] Purdue University, West Lafayette, IN, USA,
huan1368@purdue.edu, mill2459@purdue.edu, kauru@purdue.edu,
rvoyles@purdue.edu
[2] Pennsylvania State University, State College, PA, USA,
sup103@psu.edu, rxs1279@psu.edu

Abstract. Exploration of complex environments is still a challenge for real-world applications of robots. Robots that rely on locomotion modes such as wheels and treads are designed for relatively flat engineered and non-engineered surfaces and may not be suitable for operating in complex environments. Robots with hybrid modes of locomotion, such as tread/limb and tread/limb/serpentine hybrids have evolved for more aggressive and complex terrains. A problem with these highly hybridized locomotion modes is the lengthy trial-and-error process often required to develop and iterate a successful design and compatible gait strategy. We have begun using modular robotic components to quickly develop and swap modules to meet a variety of locomotion scenarios. This paper presents the development of a novel suite of modular robot components to explore locomotion strategies for some very different environments: underground corrugated drain tile and a cow's digestive chamber. The variety of robotic modules within our "bag of tricks" – some conventional and some custom-built – allow us to rapidly discover novel hybrid locomotion schemes that may not be obvious. From "wheg"-like steerable wheel/limb hybrids for drain tiles to novel buoyancy control configurations for the cow rumen, we describe the benefits of modular robots for rapid prototyping of hybrid gaits.

Keywords: modular robot, hybridized locomotion mode, buoyancy gait

1 Introduction

Exploration of inaccessible and unknown environments with robotic sensors remains a challenge in real-world applications. An example is emergency response, wherein the goal is generally to explore with cameras and sensors so human teleoperators can infer where survivors are trapped. Many such robots have been developed for various niches in this field, but only a few have received widespread use, largely because of the difficulty of locomoting through such chaotic environments. Wheels provided easy mobility around the perimeter of emergencies and in special circumstances [1] [2], but focus quickly shifted to tracked vehicles for deconstructed environments. Tracked vehicles enhance traction and stability and several commercial examples have evolved for general purpose use [3] [4] [5]. Still, tracked vehicles did not gain widespread application in complex terrains until the iRobot Packbot hybridized tracks and limbs [6]. The Packbot adds a simple, one-degree-of-freedom (DoF) "flipper" to the tracked locomotion, dramatically enhancing locomotion capability. Since then, additional hybrid locomotion modes have begun to proliferate through extensions of tread/limb hybrids [7] [8], hybrids that employ snake-like locomotion with high-DoF [9] [10], and other tread/limb/serpentine hybrids [11] [12] [13].

However, a problem with these hybridized systems has been the highly optimized and specialized designs that are costly and expertise-intensive to design. These systems are often subject to failures and cumbersome to operate due to their novel, "one-off" designs. In pursuit of the development of a wide variety of disparate miniature robotic systems, we have begun to standardize the suite of actuation modules for interchangeable use. This *familiarity through modularity* allows for more robust designs of the modules to propagate and enhances system robustness and usability, in turn. It also allows for broader and quicker exploration of the hybrid locomotion space and the resulting complexity of locomotion "gaits" that must be co-developed with the hardware. While this paper is not focused on emergency response, the expertise developed and lessons learned on those prior examples, to evolve our modular and reconfigurable system, are employed to new domains of hybrid mechanisms.

The core components that form the basis of our "Bag of Modules" are from the MOTHERSHIP (Modular Omnidirectional Terrain Handler for Emergency Response, Serpentine and Holonomic for Instantaneous Propulsion) [14] and CRAWLER (Cylindrical Robot for Autonomous Walking and Lifting for Emergency Response) [15] robots. Both of these use hybrid locomotion gaits – at the meter-scale and centimeter scale, respectively – but were developed using specialized designs. Inspired by our own work on modular real-time systems [16] we combined these diverse size scales into a common modular suite that allows the rapid prototyping of hybrid locomotion solutions to the demands of different scenarios and problems.

To highlight the benefits of modularity and interoperability, we examine two completely different applications with radically different forms of hybrid locomotion that share some modules. A new modular robot called DAUGHTERSHIP (Directional Active Underwater Gait Hybrid with Tiny Energy Reserves for Sensing Health, Inactivity and Productivity) is being developed for *in vivo* sensing of animal health in the complex, stratified liquid environment of the cow stomach. This *animal agrobot* employs a novel form of buoyancy-based locomotion to control orientation and translation of the sensor-laden DAUGHTERSHIP. Additionally, a drain tile locomotion *crop agrobot* is described to explore the soil microbiome, deep below the surface of Midwestern farms.

The contributions of this paper are:

– A bag of heterogeneous modules for rapid prototyping of hardware/software co-design techniques for hybrid locomotion gaits is proposed.
– A novel hybrid buoyancy gait for orientation and translation control in liquid environments is proposed that resulted from the demonstration.

2 Suite of Configurable Robot Modules

An eclectic suite of modular components has evolved and allows a great deal of design creativity. Due to space limitations, we describe the mini-modules in this section, detailing their locomotion and functionalities. The resulting modular configurations consist of mechanically linked steering and propulsion modules.

2.1 2-DoF Articulating Joint

With the omnidirectional characteristic enabled by the coincidentally and orthogonally placed components, this articulating joint consists of two major units: the central ring as shown in Fig.1(a) and interconnecting cable-driven housings as shown in Fig.1(b). The four posts on the outer side of the central ring enable the mounting of the housings on both sides. The coupling method between the ring and cables offers two DoF to this modular robot. Two sets of cable-driven cylinders were placed in this articulating joint, and each of them can be individually controlled by a 6 volt DC motor. The cylinders, in tandem with a cable-driven system, are designed to accommodate the actuators for the mechanisms used in each module. When assembled with a central ring, each cylinder provides one DoF, and the torque required to control the cylinders is 351 mNm. The total weight of the articulating joint is only 77 grams (dimensions: 33mm diameters, 130 mm total length). All actuators are contained within the cylinders to facilitate rotation of the joint and movement of the modular attachments. The rotation at each DoF is activated through a cable system which provides sufficient torque for movement. Full rotation from -60 °to 60 °can be attained.

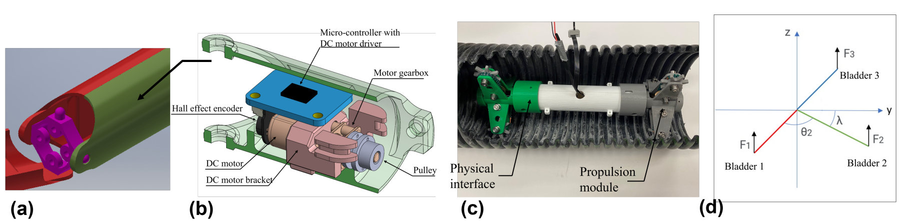

Fig. 1. Structure of articulating joint and subterranean robot. (a) The central ring design (b) The articulating joint cut-section view. (c) The subterranean robot drive through pipeline. (d) Shows the angles with respect to the buoyancy robot structure.

2.2 Wheg-Like Propulsion Module

The design of the propulsion module consists of a system of three idler gears meshing with a central worm gear, as shown in Fig.1(c). The mechanism divides one motor input into three shaft outputs and these shafts supply the relatively high torque to navigate the rough terrain we are attempting. A single worm gear divides the motor rotation among the three radially-spaced gear trains with the use of perpendicular gear meshing. Secondly, these gears are not back-drive-able, but provide the desired torque advantage. The output wheel of each gear train is a rimless multi-spoked wheel, like a Wheg [17], that engages the corrugations of the pipe with gearing traction. This wheel/leg hybrid design enables the robot to fit into corrugations in the tubing and provide enough traction to overcome large obstacles.

2.3 Buoyancy-Control Propulsion Module

This buoyancy module was developed consisting of three bladders, shown as Fig.1(d). Bladder 3 was connected orthogonally to link 2. Bladders 1 and 2 were on both sides of articulating joint. Works like ocean gliders, this module can change its buoyancy center by changing the weight of the bladders through injecting and extracting water, which will allow up-and-down movement through the water. Meanwhile, by combining the articulating joint, this buoyancy module can adjust its gesture until it comes to its static equilibrium.

2.4 Inch-Worm Propulsion Module

Peristaltic actuation is an important form of locomotion in the natural world. Earthworms and other insects (such as nematodes) use peristaltic actuation to either powerfully enlarge granular media or gently grapple fragile tissues. Hence, this peristaltic actuation is highly valuable in a reconfigurable context. Our collaborators at Penn State developed the inch-worm propulsion module described here. In Fig.2(a) a worm robot for solid surfaces is illustrated with multiple segments and its gait cycle (Fig.2(c)). The longitudinal peristaltic module uses an asymmetric frictional outer surface to inch forward, and one of the three actuation units actuates at a time. The pull force of the inch-worm module depends on the materials of interaction. When the elastomeric sheet interacts with soft silicone, as shown in Fig.2(d), the peak propulsion force is up to 10 N.

3 Example Problem Scenarios for Robotic Sensing

3.1 In Vivo Sensing of Rumen Digestive State

A cow's digestive chamber, or rumen, is a large organ wherein the feed is digested and converted by bacteria into proteins and energy through fermentation. The liquid in the rumen is a highly stratified environment with a thick mat of feed on the top, followed by fluid with suspended particles, but it is stirred occasionally

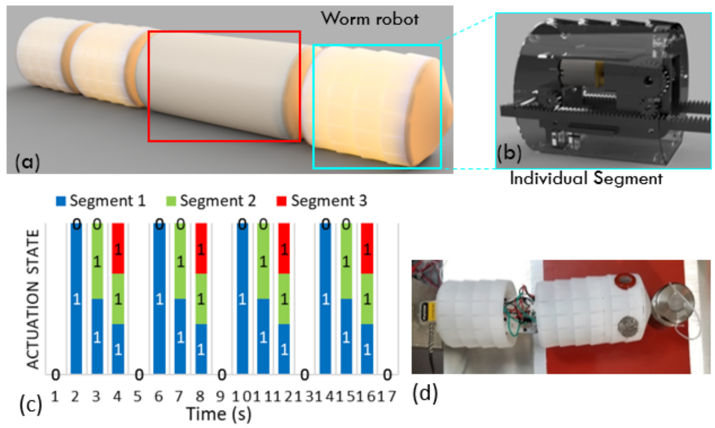

Fig. 2. Inch Worm propulsion module, (a) multi-segment robot with articulating joint (red) and peristaltic module (cyan) (b) individual longitudinal peristaltic segment, (c) actuation gait of worm robot, and (d) module drawbar test.

by contraction. The volume of the rumen is 184 liters and the lining is populated with colonies of micro-organisms that aid in digestion of the food. In order to monitor the digestion and rumen health, animal nutritionists are using boluses to take measurements of rumen environment such as volatile fatty acids (VFA), pH, temperature, etc. However, boluses are stationary sensor packs settled at the bottom of the rumen which fails to capture the health changes occurring at various levels of this highly complex environment. An in-vivo explorer robot with locomotion capabilities can overcome this limitation, creating a new dimension of understanding of the function of the rumen and its correlation with the overall health of the animal.

3.2 Subterranean Exploration of the Soil Microbiome

Underground agricultural drain pipes are corrugated plastic pipes used for insuring the soil of the farmland remains free of excess water. They are essential for farming yet often face issues associated with blockage due to weeds and debris falling in. They are mostly laid straight with few T-intersections. Inspection robots are needed in such an environment to sense gas and water content to monitor the nutrients in runoff as well as to identify any blockage. However, these toothed pipelines have proved to be difficult terrain for wheeled robots. Thus, hybridization of wheels and limbs (e.g. gears) helps to improve the performance of locomotion. Some hybrid robots, like leg-wheeled hybrid robots and wheeled-tracked hybrid robots, represent the next step in hybridization as they combine wheels, tracks, and limbs to develop a giant leap in mobility.

4 Hybrid Locomotion Gaits

The hybrid locomotion modules enable the robot to display a better performance in an amphibious environment. By mounting it with different modules, this modular robot can achieve a wide variety of motions and gaits corresponding to the module's design for use in a given environment.

4.1 Motion Analysis of Buoyancy Modules

In the buoyancy robot, the angles between links are geometrically related. As shown in Fig. 1(d), let θ_1 and θ_2 be the rotation angles around Pitch axis and Yaw axis, respectively. Let ϕ_1, ϕ_2, and ϕ_3 be the angles between the three links and the vertical plane (YOZ plane). Based on the mechanism, link 2 and link 3 are normal to each other. The sum of θ_1, ϕ_1, and ϕ_2 equals to π. Thus, θ_1, ϕ_1, ϕ_2, and ϕ_3 can be calculated with the equations (1) and (2).

$$\phi_2 + \phi_3 = 90^\circ \tag{1}$$

$$\phi_1 + \phi_2 + \theta_1 = 180^\circ \tag{2}$$

Let F_1, F_2, and F_3 represent the buoyancy force of these three buoyancy bladders. Let r_1, r_2, and r_3 be the lengths of the three links. Let λ be the angle between link2 and the horizontal plane (XOY plane). The value of $\phi_i s$ depends upon the frame of reference and the given value of θ_1. To match the simplified simulation, ϕ_2 is a fixed angle. When at a neutral buoyant state, the bladders provide upwards buoyancy force equaled to gravity to this robot. The steady-state equilibrium can be expressed as:

$$\sum \tau = r_i(\theta_1, \theta_2, \lambda, \phi_1, \phi_2, \phi_3) \times F_i \tag{3}$$

The equation suggests that equilibrium is decided by the angle of articulating joint and buoyancy force of each bladder when other parameters are constant. In this situation, λ can be calculated as:

$$\tan \lambda = \frac{F_3 \sin \phi_3 - F_2 \sin \phi_2 + F_1 \cos \theta_2 \sin \phi_1}{-F_1 \sin \theta_2 \sin \phi_1} \tag{4}$$

When θ_1 and θ_2 are fixed, changing the mass of the robot yields the unbalance between gravity and buoyancy force, which becomes the power source of the robot's movement. In this scenario, any transformation of this robot will cause the stable orientation shift, causing the robot to settle into a new stable position.

4.2 Novel Buoyancy Gaits

In the simplest case, the concept of a "buoyancy gait" is more about the change of orientation. In its neutrally buoyant state, any changes to the robot's gesture will cause movements that disrupt its condition. The altitude of the three bladders automatically adjusts to keep the equilibrium as the robot makes gestures. Meanwhile, by carefully shaping the bladders – using them as hydrofoils – changes can be made not only on orientation but on the lateral position. However, all the activities are happening inside the ruminal cavity, which is undergoing periodic contractions. It had not been determined if these “gaits” will counteract the effects of the contractions, but capturing the currents caused by these contractions – effectively “riding the waves,” is the next step. For this paper, we focus only on motion in the still fluids between contractions, as this is when we want to sense the strata of the rumen.

According to equation (3), F_i is the only parameter that can influence the robot's locomotion once the θ_1 and θ_2 are settled. The buoyancy gait of this modular robot is correlated with its bladders' buoyancy force changes. If the masses of these three bladders proportionally reduce or increase during a certain process, the buoyancy gait for the robot will be either vertically floating or vertical sinking, ideally. However, this vertical movement is not stable due to the influence of water flows generated by robot motion, and achieving a precisely proportional mass changing may also be a challenge for encoders. Thus, adjusting the masses for three bladders with keeping the robot in a neutral configuration has been a new solution for controlling the robot's orientation. According to equation (4), when the robot suspends inside the water with constant weight and fixed rotation angles, attitude is affected by three buoyancy forces. In order to keep the final total water content unaltered, when water is separately pumped from or injected into the bladders, the robot will have motions to keep its balance due to the unbalance between gravity and buoyancy force. The final depth of the robot is immobile due to the constant nature of gravity, but the joint position will be adjusted in order to facilitate a stable configuration at the stable depth. In the same way as F_i parameter, parameters θ_1 and θ_2 are factors that can influence the robot's attitude. Varying rotation angles lead the robot to have different postures as well as predictable motions which can be calculated by the steady-state equilibrium. Also, bladders with oblate shapes functioning like flippers can improve the performance on the orientation control by utilizing the fluid's characteristics.

4.3 Adaptive Cyclic Pattern Generator for Subterranean Steering

Like a subway tube, the drain tile provides a guide way to steer the robot along the length of the buried pipe as the Wheg propulsion units propel it forward or backward. However, some sections of the buried drain tile may have “Y-” and “T-intersections.” Placing the articulating joint between two propulsion modules enables the subterranean robot to make selective turns to visit different parts of the field. This combination of articulating joint and propulsion modules requires coordination of both the front and rear drive modules. In general, the two propulsion modules are in sync – running at the same frequency and in phase – and driven by a single central pattern generator (CPG) [18] that keeps the individual Whegs from conflicting with one another. But when turning with the articulating joint in the center, the front propulsion module begins to cross the corrugations at an angle, elongating the spatial frequency of Wheg engagements with the corrugations. The CPG, then, uses steering commands to shift the frequency of the steering module in relation to the rear module.

A CPG also controls the inch-worm gait for the non-liquid agRobot locomotor, as indicated in Fig 2(c). The inch-worm peristaltic CPG is not adaptive, as steering does not impact the propulsion sequence.

5 Experimental Results

A transparent water container (dimensions: 584mm length, 432mm width, and 305mm height) was used as the underwater environment. Two fixed cameras captured the top view and side view. Initially, the robot stays neutrally buoyant without any disturbance. The joint angle was controlled, and the rotation angles θ_1, θ_2 were subsequently measured when the robot floated to its equilibrium orientation in the water. Fig. 3 showed the buoyancy motion at various rotation angles in the experiment.

Initially, the robot was suspended underwater with neutral buoyancy when θ_1 equals 160°. Maintaining θ_1 as a fixed rotation angle we then assigned different rotation angles to θ_2 (150°, 160°, 170°, 180°) to observe the locomotion of the buoyancy module. Since θ_1 was fixed, no significant gestures change can be observed from the top view. Thus, the result of buoyancy gaits was presented by the rotation angle captured from the side view. There were two variables in this experiment, mass (F_i) and rotation angle (θ_2), and we tested them separately. Based on the fixed angle of θ_2, we changed the weight of three bladders but kept the total weight unchanged. For rotation angle testing, we kept each bladder's weight constant but let the robot settle to the given angle and captured their neutral state. According to Fig. 3(a) and Fig. 3(b), the gesture of the robot was changed when each bladder mass was changed under the circumstance of unchanged total weight and fixed θ_2 angle. From the figures, as we properly reduced the weight for link 1 but increased the same for link 3, bladder 1 was visibly elevated. According to Fig. 3(c)-(f), based on the unchanged weight of bladders, the robot's gesture was changed due to different rotation angle θ_2. Table 1 presents the results of both the predicted angles from the simulation and the actual angles we obtained from the experiments.

Table 1. Angles of robot joints from simulation and test

θ_2 angle	predicted λ	actual λ
150°	60°	66°
160°	52°	53°
170°	48°	50°
180°	38°	40°

Results showed the ability of this simulation to predict the orientation for a real underwater robot even though the environment for this modular robot

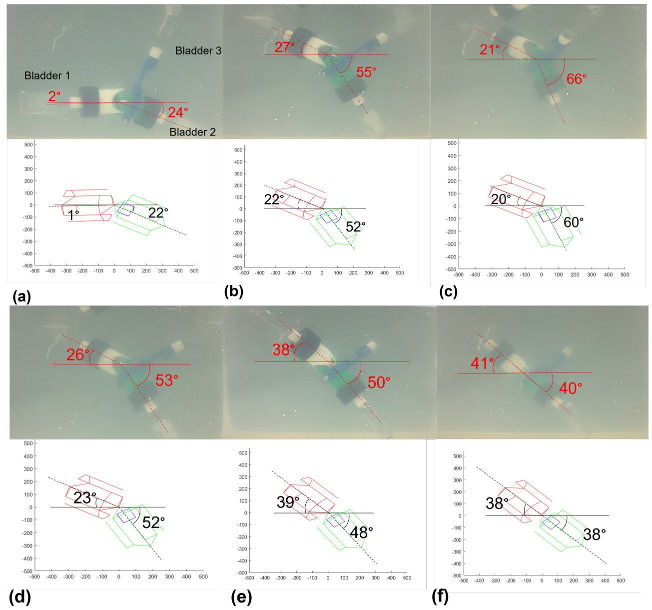

Fig. 3. (a) Neutral state of buoyancy robot ($\theta_2 = 160°$) (b) Neutral state of buoyancy robot with adjusted bladder mass ($\theta_2 = 160°$). (c)-(f) Neutral state of buoyancy robot given different θ_2 angles.

is complicated and there exists variance between the simulation and measured orientation angles.

6 Conclusions and Future work

This paper proposed a suite of modular robot components for the rapid prototyping and testing of hybrid forms of locomotion in highly specialized environments. This work introduced the advantages of using a modular robot with hybrid gaits in the field of robotics. A pipeline traversing modular robot with "wheg" locomotion was built with an adaptive CPG-based gait controller. The robot can move forward through and around corners in corrugated drain pipe. This modular robot has a compact structure, low production cost, and high controllability. We also presented the novel hybridized buoyancy gait. We have proven the effectiveness of the novel gaits that were co-developed with the system in simulated and real-world experiments. Furthermore, these robots are adaptable to complex working environments and capable of quickly switching modules to meet varieties of requirements. Because of the modular design of this robot, it can be quickly repaired by replacing the same modules, which increases the feasibility of the robot in practical application. The further study will focus on exploring buoyancy force control. Soft materials will be considered for our future research and we aim to embed sensors on the soft material to enrich the robot's functionality.

7 Acknowledgements

The authors would like to thank the USDA/NIFA for support of this work through grants 2019-67021-28990 (1018075) and 2019-67021-28991 (1018631).

References

1. A. Morris, D. Ferguson, Z. Omohundro, D. Bradley, D. Silver, C. Baker, W. Whittaker (2006). "Recent developments in subterranean robotics." Journal of Field Robotics, 23(1), 35-57.
2. J. Abouaf, "Trial by fire: teleoperated robot targets Chernobyl," in IEEE Computer Graphics and Applications, vol. 18, no. 4, pp. 10-14, July-Aug. 1998.
3. "Bomb Disposal Robot - QinetiQ." https://www.qinetiq.com/en-us/capabilities /robotics-and-autonomy/talon-medium-sized-tactical-robot (acc: Apr. 13, 2021).
4. R. R. Murphy, J. Kravitz, K. Peligren, J. Milward and J. Stanway, "Preliminary report: Rescue robot at Crandall Canyon, Utah, mine disaster," 2008 IEEE International Conference on Robotics and Automation, 2008, pp. 2205-2206.
5. M.J. Micire (2008), "Evolution and field performance of a rescue robot." J. Field Robotics, 25: 17-30.
6. "PackBot - ROBOTS: Your Guide to the World of Robotics." https://robots.ieee.org/robots/packbot/ (accessed Apr. 06, 2021).
7. T. Yoshida, K. Nagatani, S. Tadokoro, T. Nishimura, and E. Koyanagi, "Improvements to the rescue robot quince toward future indoor surveillance missions in the Fukushima Daiichi nuclear power plant," in Springer Tracts in Advanced Robotics, 2014, vol. 92, pp. 19–32
8. W. A. Lewinger, C. M. Harley, R. E. Ritzmann, M. S. Branicky and R. D. Quinn, "Insect-like Antenna Sensing for Climbing and Tunneling Behavior in a Biologically-inspired Mobile Robot," IEEE Intl. Conf. on Rob. and Auto., 2005, pp. 4176-4181.
9. J. Whitman, N. Zevallos, M. Travers and H. Choset, "Snake Robot Urban Search After the 2017 Mexico City Earthquake," IEEE Intl. Symp. on Safety, Security, and Rescue Robotics (SSRR), 2018, pp. 1-6
10. R. Ariizumi and F. Matsuno, "Dynamic Analysis of Three Snake Robot Gaits," in IEEE Transactions on Robotics, vol. 33, no. 5, pp. 1075-1087, Oct. 2017
11. J. T. Lane and R. M. Voyles, "A 2-D tread mechanism for hybridization in USAR robotics," IEEE Intl. Symp. on Safety, Security, and Rescue Robotics (SSRR), 2016.
12. A. Masayuki, T. Takayama and S. Hirose, "Development of "Souryu-III": connected crawler vehicle for inspection inside narrow and winding spaces," IEEE/RSJ Intl. Conf. on Intelligent Robots and Systems (IROS), 2004, pp. 52-57 vol.1.
13. J. Borenstein and A. Borrell, "The OmniTread OT-4 serpentine robot," IEEE Intl. Conf. on Robotics and Automation, 2008, pp. 1766-1767.
14. J. Huff, S. Conyers and R. Voyles, "MOTHERSHIP — A serpentine tread/limb hybrid marsupial robot for USAR," IEEE Intl. Symp. on Safety, Security, and Rescue Robotics (SSRR), 2012, pp. 1-7
15. R. M. Voyles and R. Godzdanker, "Side-Slipping Locomotion of a Miniature, Reconfigurable Limb/Tread Hybrid Robot," IEEE Intl. Wkshp. on Safety, Security and Rescue Robotics, 2008, pp. 58-64
16. Y Cui, RM Voyles, JT Lane, A Krishnamoorthy, MH Mahoor, "A mechanism for real-time decision making and system maintenance for resource constrained robotic systems through ReFrESH," in Autonomous Robots 39 (4), 487-502, 2015.

17. A. S. Boxerbaum, J. Oro and R. D. Quinn, "Introducing DAGSI Whegs™: The latest generation of Whegs™ robots, featuring a passive-compliant body joint," IEEE Intl. Conf. on Robotics and Automation, 2008, pp. 1783-1784.
18. B. R. Tietz, R. W. Carnahan, R. J. Bachmann, R. D. Quinn and V. SunSpiral, "Tetraspine: Robust terrain handling on a tensegrity robot using central pattern generators," IEEE/ASME Intl. Conf. on Adv. Intell. Mecha., 2013, pp. 261-267.